Detecting Snow in Western New York and Eastern California using Sentinel-1a SAR and VIS/NIR Snow-Cover Maps

DOROTHY K. HALL[1,2], NICOLO E. DIGIROLAMO[2,3], AND GEORGE A. RIGGS[2,3]

ABSTRACT

Knowledge of the amount of snow and timing of snowmelt allows reservoir managers to optimize use of water resources and to improve predictions of water availability. With the currently available spaceborne visible/near-infrared (VIS/NIR) and synthetic aperture radar (SAR) satellite data, it is possible to map snow cover and to delineate areas of wet snow under certain circumstances. A great advantage of using SAR data for snow mapping is that data acquisition is unaffected by non-precipitating clouds, in contrast to VIS/NIR derived data products that can only image the surface under clear skies. The objective of this work was to determine the utility of Sentinel-1a (S-1a) C-band SAR data when used in combination with available snow-map products for mapping snow in western New York state and in a mountainous area in eastern California (Sierra Nevada (SN) mts.). We selected an initial study period from 1 December 2022 through 31 January 2023 for this analysis. In both study areas, using a time series of S-1a C-band SAR backscatter images, there were no significant backscatter, σ^0, changes indicating the presence of snow cover even when the VIS/NIR satellite snow-cover maps showed snow cover. The presence of cropland and deciduous forests in combination with the thin (generally < ~0.1 m), wet snow cover likely prevented the C-band SAR from detecting snow in the western New York study area. In the SN mts. study area during this time period, an expected decline in σ^0 as the snowpack developed was not observed. Further analysis of the SN snowpack was conducted during active melting in May of 2023 revealing a drop in σ^0 of up to ~4 dB as the melting progressed. Though promising, we consider these results to be preliminary because more data during the SN melting period are needed. Backscatter from snow at X/Ku-band is up to 40 times stronger compared to C-band and thus shows a great deal more potential for mapping both dry and wet snow as compared to C-band.

INTRODUCTION

Knowledge of the amount of snow and timing of snowmelt allows managers to optimize use of water resources and to improve predictions of water availability. When a snowpack becomes wet, melting may be imminent. With spaceborne visible/near-infrared (VIS/NIR) and synthetic aperture radar (SAR) data, it is possible to map snow cover and to delineate areas of wet snow, especially when meteorological station data are also available.

The objective of this work was to determine the utility of Sentinel-1a (S-1a) C-band SAR data used in combination with available snow-map products for mapping snow in western New York

[1] Earth System Science Interdisciplinary Center / University of Maryland, College Park, MD, USA
[2] Cryospheric Sciences Lab / NASA / Goddard Space Flight Center, Greenbelt, MD, USA
[3] SSAI, Lanham, MD, USA
Corresponding author: dkhall1@umd.edu

state and in the Sierra Nevada (SN) Mountains in eastern California. S-1a C-band SAR data have been shown to be useful for mapping wet snow when used in conjunction with VIS/NIR snow maps (e.g., Nagler et al., 2016; Solberg et al., 2016). A great advantage of using SAR data for snow mapping is that acquisition of data is unaffected by non-precipitating clouds, in contrast with use of visible/near-infrared (VIS/NIR) derived data products that can only image the surface under clear-sky conditions. Thus, a determination of the utility of available SAR data for mapping snow is important because of the predominance of clouds over so many areas of North America when snow is on the ground. Initially, we selected a study period from 1 December 2022 through 31 January 2023 for this analysis, but then added a second study period, 1 April – 10 May 2023, for the SN study area to investigate the C-band SAR response during spring melting.

We used snow map data products derived from the MODerate-resolution Imaging Spectro-radiometer (MODIS) instruments on the Terra and Aqua satellites and the Suomi National Polar-orbiting Partnership (*NPP*) satellite, along with backscatter, σ^0, maps from the European Space Agency's (ESA's) S-1a C-band SAR (ESA, 2023).

STUDY AREAS

Western New York State

The New York study area (Fig. 1) is located in an area of western New York state that is predominantly cloudy for much of the fall and winter seasons.

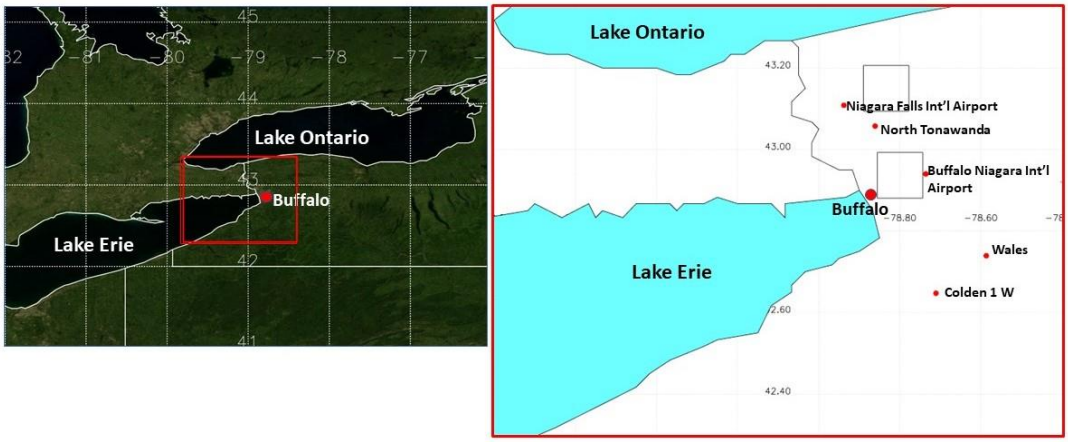

Figure 1. Left Panel - NASA Worldview base image showing the location of the study area in western New York state outlined in red (from the Blue Marble overlay based on an August 2004 shaded relief map (GIBS, 2004)). Right Panel– Zoom of study area. Locations of five meteorological stations are shown as red dots. The approximate location of the city of Buffalo, NY, is shown as a large red dot.

The New York study area is composed of croplands in the northern part and largely deciduous broadleaf forests in the southern part according to the 500-m resolution yearly MODIS-derived land-cover product, MODIS/Terra+Aqua Land Cover Type, MCD12Q1 (Friedl and Sulla-Menashe, 2019) (Fig. 2).

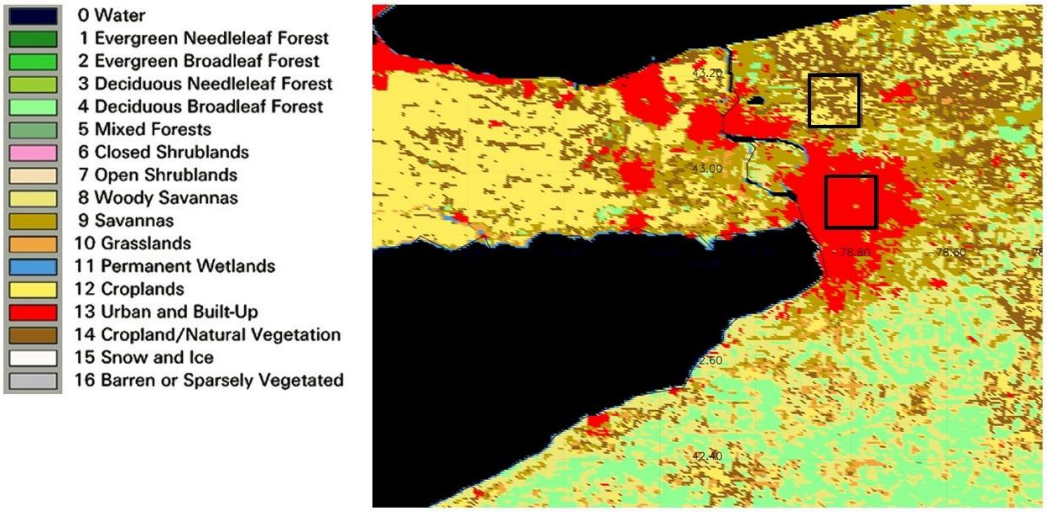

Figure 2. MODIS/Terra+Aqua Land Cover Type Yearly L3 map for 2021 MODIS/Terra+Aqua Land Cover Type, MCD12Q1 (Friedl and Sulla-Menashe, 2019) covering the study area shown in the right panel of Fig. 1. MCD12Q1 is based on the IGBP global vegetation classification scheme.

Sierra Nevada Mountains, California

The California study area (Fig. 3) is intermittently cloudy for much of the fall and winter seasons. It is composed of cropland, evergreen needleleaf forests and other according to the 500-m resolution yearly MODIS-derived land-cover product, MODIS/Terra+Aqua Land Cover Type, MCD12Q1 (Friedl and Sulla-Menashe, 2019) (Fig. 4). The highest elevation in the SN Mts. is ~4420 m.

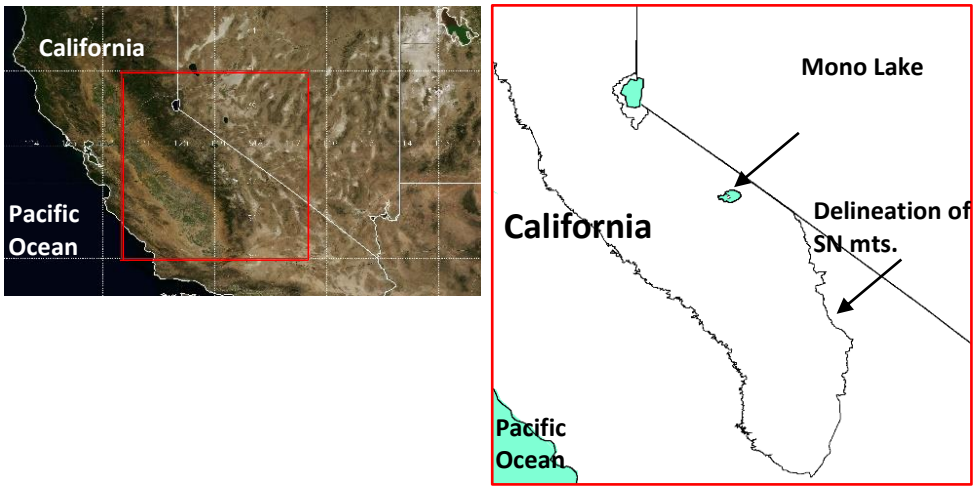

Figure 3. Left Panel - NASA Worldview base image showing the location of the study area in California outlined in red from the Blue Marble overlay based on an August 2004 shaded relief map (GIBS, 2004). Right Panel – Zoom of study area. The straight black lines delineate the California/Nevada border and the Sierra Nevada mts. are delineated using a shape file (see: https://sierranevada.ca.gov https://snc.maps.arcgis.com/home/webmap/viewer.html?webmap=66bb667660cb40b4a5b807192466f33d).

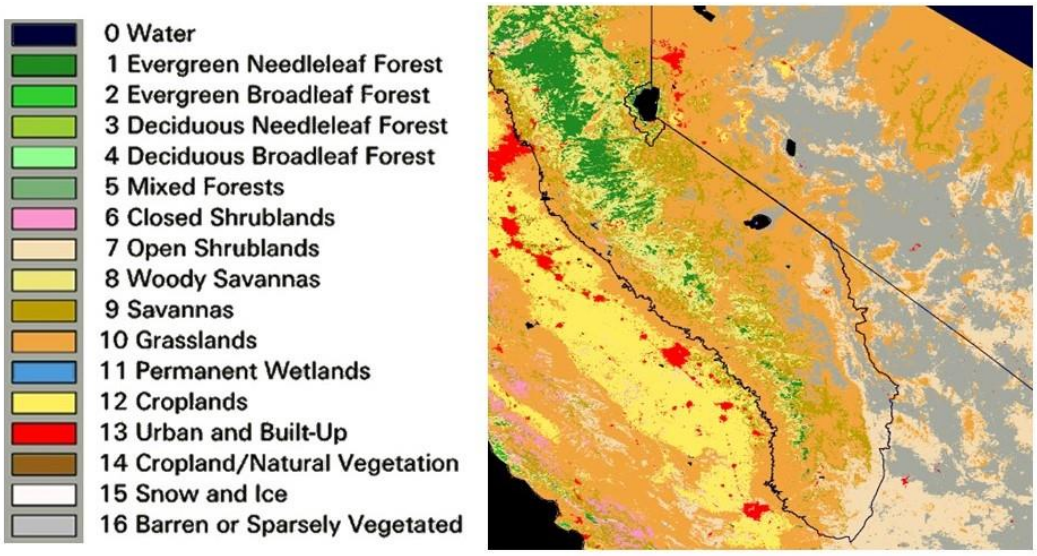

Figure 4. MODIS/Terra+Aqua Land Cover Type Yearly L3 map for 2021 MODIS/Terra+Aqua Land Cover Type, MCD12Q1 (Friedl and Sulla-Menashe, 2019) covering the study area shown in the right panel in Fig. 3. MCD12Q1 is based on the IGBP global vegetation classification scheme.

DATA

Snow-Cover Data Products

NASA standard snow-cover extent (SCE) data products, MOD10A1F and MYD10A1F, from the MODIS Terra and Aqua satellites, respectively (Hall and Riggs, 2020) and VNP10A1F from the Suomi National Polar Platform (SNPP) (Riggs et al., 2019) were used to map snow cover in the study areas. The MODIS and VIIRS data products were developed using a cloud-gap filling (CGF) algorithm, the details of which may be found elsewhere (Riggs et al. 2019 and Riggs & Hall, 2021). The accuracy of the CGF MODIS and VIIRS data products is compromised under persistently-cloudy conditions such as are found in the New York study area during late fall and winter seasons; for more accurate mapping, periodic views of the surface are needed to update the fully-automated snow decisions. Therefore, we also used the partially-automated Interactive Multisensor Snow and Ice Mapping System (IMS) 4-km resolution snow maps that are developed using a variety of satellite and station information and updated daily by trained meteorologists (Helfrich et al., 2018); IMS SCE maps are less affected by cloud-cover conditions on any given day than are the MODIS- and VIIRS-derived SCE maps.

There is a great deal of literature about the MODIS and IMS snow-cover products that will not be reviewed here. The MODIS SCE products have been available since February of 2000 and are produced in a completely automated computing environment. There have been several "collections," or versions of the MODIS SCE algorithms, each one providing improvements over the previous one. The current collection is Collection 6.1, or C6.1. The NASA VIIRS snow-cover products are modeled after the MODIS products, so details are not repeated here, but may be found in the user guides (Riggs et al., 2019; Riggs and Hall, 2021). We used the NASA VIIRS Collection 2 (C2) data products available from the National Snow and Ice Data Center (NSIDC, 2023).

Meteorological Station Data

All meteorological data used herein were obtained from NOAA (NCEI, 2023) or from the USDA (SNOTEL, 2022 - 2023). Five meteorological stations in New York were selected (Fig. 1 - right panel): Buffalo Niagara International Airport, Colden 1 W, Niagara Falls International Airport, North Tonawanda and Wales. For the SN study area, only the Virginia Lakes Ridge SNOTEL station in California was used; it is located to the north of Mono Lake in California (Fig. 5). We

plotted the maximum (Tmax) and minimum (Tmin) daily air temperatures and snow depth during snowmelt in the months of April and May 2023. Using air temperature information, we estimated the state (wet vs dry) of the Sierra Nevada snowpack.

Figure 5. NASA Worldview image, 13 May 2023, showing Mono Lake in the central SN mts., eastern California. Mono Basin is outlined in black. The red dot to the north of the lake is the approximate location of the Virginia Lakes Ridge meteorological station.

Sentinel-1a

The S-1a satellite has a C-band SAR instrument on-board that was launched on 3 April 2014 with a repeat cycle of 12 days (ESA, 2023). We used the Interferometric Wide Swath (IW) mode, with VV+VH polarizations. IW is the nominal operation mode for land areas. The C-band SAR operates at a center frequency of 5.407 GHz, and has a swath width of 250 km and a nominal resolution of 5 m X 20 m. Details about the S-1a SAR may be found elsewhere (ESA, 2023).

For the New York study area, we used σ^0 maps derived from the C-band SAR acquired on 10 & 22 December 2022 and 3, 15 & 27 January 2023. The 10 December 2022 SAR σ^0 map was used as a snow-free reference map. For the California study area, we used σ^0 images from 8 December 2022 and 25 January 2023 as well as a snow-free reference image from 28 October 2022. Additionally, for the SN study area, we downloaded two S-1a SAR images acquired during active melting in the spring. The dates of the spring SAR images are: 8 & 13 May 2023.

Using S-1a C-band SAR to Identify Areas of Wet Snow

In earlier work (see Bernier and Fortin, 1998; Bernier et al., 1999; Baghdadi et al., 2000) it was reported that both wet and dry snow could be mapped successfully using C-band Radarsat data and even that snow-water equivalent (SWE) could be estimated (Bernier et al., 1999). However in recent literature, it has not been corroborated (to our knowledge) that C-band SAR data, for example from the S-1a satellite, is universally useful for determination of SWE, though Lievens et al. (2019) have reported success in mapping snow depth in deep snow in mountainous areas with S-1a C-band SAR data.

The combined use of data from optical and SAR sensors may enable the mapping of total snow area and monitoring of the temporal dynamics of snowmelt as described by Nagler et al. (2008 & 2016). Reduction of the backscattering coefficient, σ^0, in wet snow land surfaces compared to surfaces covered by dry snow or no snow is the basis for mapping wet snow areas with C-band SAR. A 3-dB threshold drop between non-snow-covered area or dry snow and wet snow has been noted in numerous works (e.g., Nagler et al., 2008; Lund et al., 2022; Solberg et al., 2016; Marin et al., 2020; and Manickam and Barros, 2020). Wet snow may be detected in a SAR image by comparing the σ^0 values with σ^0 from a reference image or images obtained during snow free or dry snow conditions (Nagler and Rott, 2000; Nagler et al., 2016). By using the average of two or more maps as a reference map, the classification accuracy can be improved (Nagler et al., 2008). Solberg et al. (2016) found a threshold of -3 dB for identifying wet snow using both C-band HH Radarsat (5.3 cm

wavelength) and C-band VV ERS-SAR data. They used both SAR signatures and backscatter modeling to develop an algorithm for mapping wet snow in mountainous areas.

Marin et al. (2020) and Lund et al. (2022) compared S-1a backscatter with *in situ*-derived snow properties and snow model simulations. Marin et al. (2020) noted a decrease in C-band SAR σ^0 as soon as liquid water appeared in the snowpack. Lund et al. (2022) found thresholds of -2 to -3 dB to identify wet snow for co-polarized S-1a C-band SAR σ^0. To compare with the SAR-derived results, they used the SnowModel to provide an independent estimate of snowpack conditions. They also used >50 snow pit observations during the 2020 SnowEx experiment in Grand Mesa, Colorado, USA, for validation and concluded that C-band SAR is a reliable method to detect meltwater in a snowpack; (Lund et al., 2022).

For wet snow the radar signal at C-band frequencies is reflected and scattered at the surface and within the top few centimeters of the snowpack, whereas in the case of dry seasonal snow, a large part of the backscatter is contributed by the snow/ground interface (e.g., see Rott et al., 1992). For wet snow with liquid water content of 5% by volume, the penetration depth is only ~3 cm at C-band (Matzler, 1987; Nagler et al., 2016).

METHODOLOGY

For each study area, we compared the daily MODIS, VIIRS and IMS SCE maps for the study period from 1 December 2022 through 31 January 2023. Because of the persistent clouds in western New York during the study period, we used the IMS daily SCE to map the snow. For the eastern California/SN study area there were frequent views of the surface thus we were able to use the higher-resolution MODIS and VIIRS daily cloud-gap-filled snow maps to map the snow.

Next, we developed S-1a C-band σ^0 reference maps from scenes acquired when there was no snow on the ground as determined from MODIS, VIIRS and IMS SCE snow maps and NASA Worldview (2022-2023). For the western New York study area, an S-1a SAR scene from 10 December 2022 was used as the reference because we were able to confirm that there was no snow on the ground on that date. For the California/Sierra Nevada mts. study area, an S-1a-SAR scene from 28 October 2022 was used because there was no snow in the mountains visible on Worldview or the VIS/NIR snow products on that date.

We plotted the maximum and minimum daily air temperatures for each of the stations for the months of December 2022 and January 2023. Using air temperature data, we estimated the state (wet or frozen) of the snowpack surface. Because of the time of SAR image acquisition (~6PM local time), we used the maximum air temperature reported on that day as an indicator of the state of the snow surface. Using the above-mentioned methodology, we estimated the snow conditions on each date on which a SAR σ^0 map was available as seen in Tables 1 & 2.

Table 1. Determination of snow presence and state (wet or frozen) for each day on which an S-1a C-band SAR image was available for the western New York study area.

Date (and time in local time) of SAR image acquisition	Snow or no snow in scene	State of the snowpack at the time of SAR data acquisition
10 December 2022 (6:08 PM)	no snow	n/a
22 December 2022 (6:08 PM)	snow	wet
03 January 2023 (6:08 PM)	no snow	n/a
15 January 2023 (6:08 PM)	snow	frozen
27 January 2023 (6:08 PM)	snow	frozen

Table 2. Determination of snow presence and state (frozen or wet) of S-1a C-band SAR images for the Sierra Nevada Mts. study area. Other dates were downloaded but not used due to time constraints.

Date (and time in local time) of SAR image acquisition	Snow or no snow in scene	State of the snowpack at the time of SAR data acquisition
28 October 2022 (6:08 PM)	no snow	n/a
03 December 2022 (6:08 PM)	snow	unknown
20 January 2023 (6:08 PM)	snow	presumably frozen
08 May 2023 (6:08 PM)	snow	wet/melting

RESULTS

For each area, we show daily SCE for the study period from 1 December 2022 through 31 January 2023. Because of the persistently-cloudy conditions in western New York state during fall and winter, we used IMS SCE maps (Fig. 6). For the SN study area for which there were frequent views of the surface during the fall, winter and spring, we show VIIRS VNP10A1F SCE CGF maps (Fig. 7).

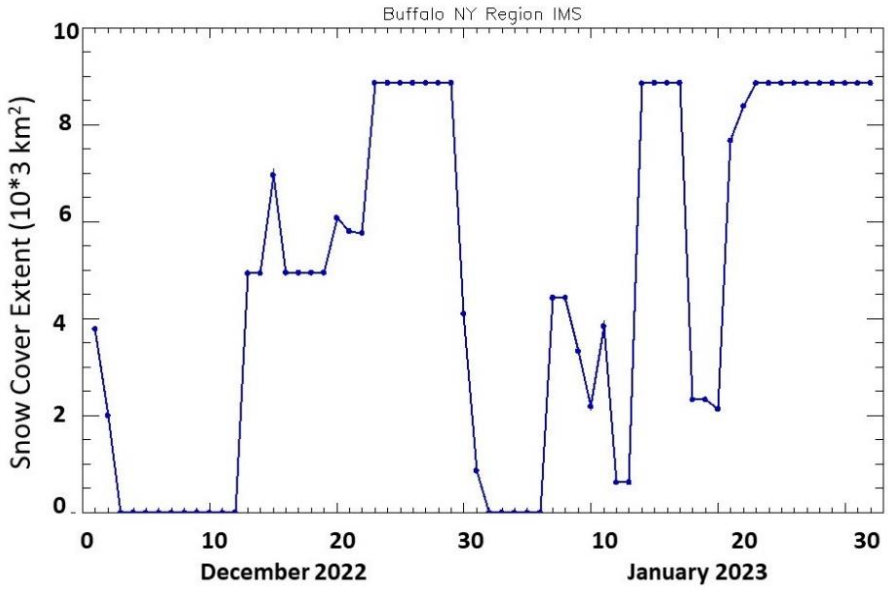

Figure 6. Daily SCE (in km^2) derived from the NOAA IMS daily snow maps in the western New York study area.

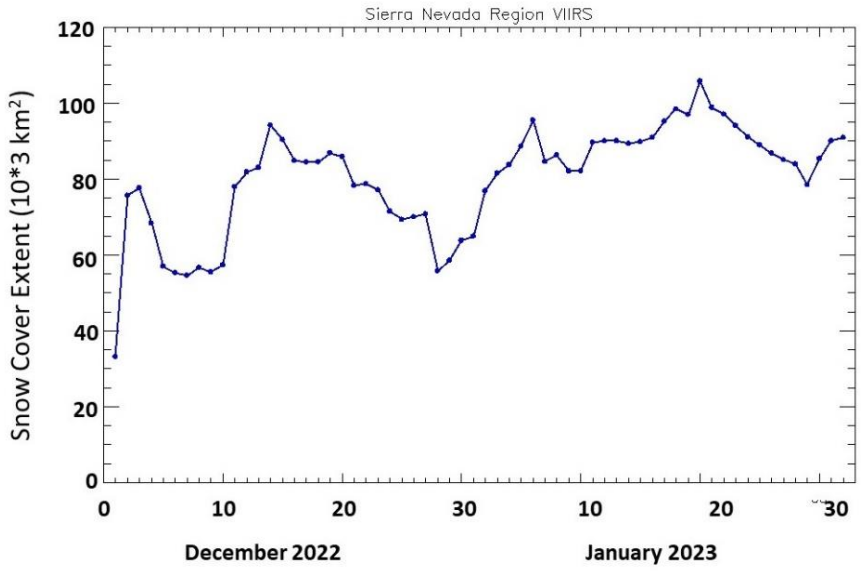

Figure 7. Daily SCE (in km^2) derived from NASA VIIRS VNP10A1F daily snow maps in the Sierra Nevada mts. study area.

Western New York study Area

From 1 December 2022 – 31 January 2023, we plotted Tmax, Tmin and snow depth from each of the five stations. An example from the North Tonawanda, NY, station is shown in Fig. 8.

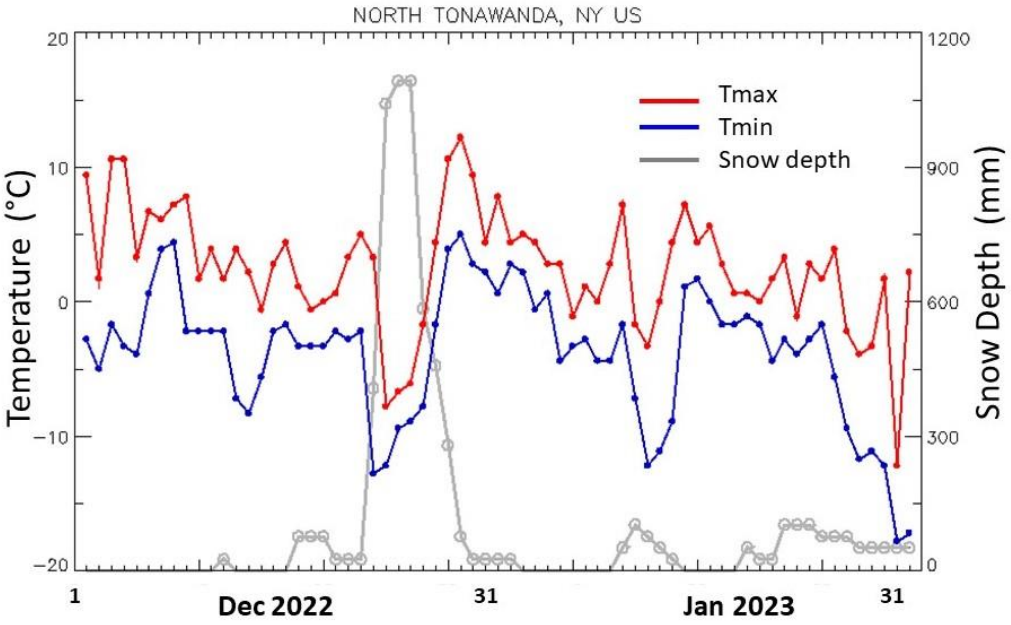

Figure 8. Daily Tmax and Tmin air temperatures (°C) and daily snow depths (mm) at North Tonawanda, NY, for the months of December 2022 and January 2023. Data were acquired from NCEI (2023).

In the land areas of the western New York study area, we did not find a significant difference in σ^0 on 22 December 2022 (when very thin snow was present (Fig. 8)) as compared to the reference image (10 Dec 2022 – not shown). Nor did we find a significant difference in the backscatter above and below the snowline on the 22 December 2022 cross-polarized SAR scene (Fig. 9a). The mean σ^0 of the land areas above (non-snow) and below (snow covered) the snowline on 22 December is -15.7515 dB, and -15.6401 dB, respectively. It is likely that the non-snow-covered land to the north of Lake Erie is wet (see Tmax in Fig. 8). It is difficult to distinguish between wet ground and wet snow using C-band SAR especially when the snow cover is thin (e.g., Nagler et al., 2016). Though the snow was deeper (up to >~ 1 m) between 23 and 31 December 2022 (Fig. 8), no S-1 C-band SAR images were available during this time period to assess the S-1a σ^0 in the deeper, wet snow.

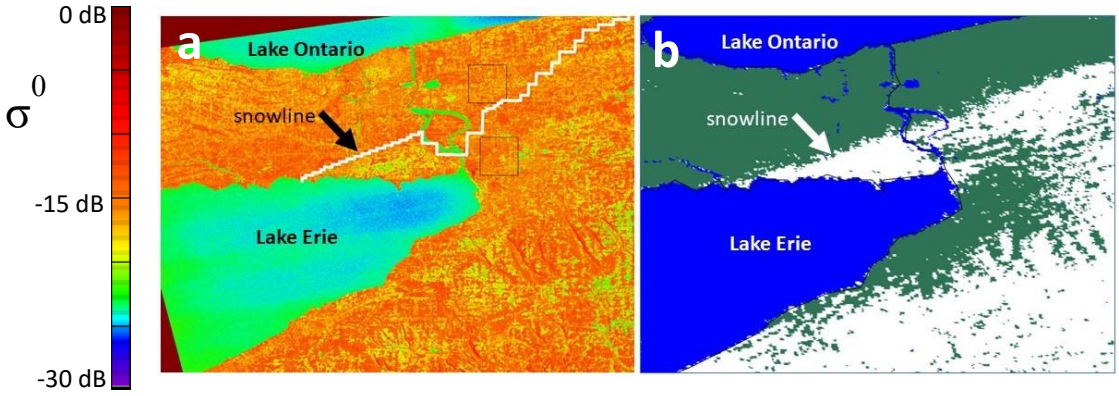

Figure 9. a) 22 December 2022 VH SAR σ^0 image. The snowline shown was derived from the 22 December 2022 IMS SCE map. b) 22 December 2022 VIIRS VNP10A1F snow map of the same area shown in the SAR image.

Sierra Nevada (SN) Mts. Area

For the Virginia Lakes Ridge SNOTEL station near Mono Lake in the SN mts., we plotted Tmax, Tmin and snow depth. Fig. 10 shows an example plot during the melt season, from 1 April – 10 May. During this time the snow was actively melting (as seen in the light blue line showing decline in snow depth).

The building snowpack in December 2022 and January 2023 did not produce significant differences in σ^0 as compared to the 28 October 2022 non-snow-covered reference image. We also developed a time series during active melting, 1 April – 10 May 2023. During active snowmelt in May 2023, the C-band SAR VV and VH σ^0 displayed a mean drop of up to 4.1 dB, within the land area of the Mono Lake Basin (Mono Basin) compared to a January 2023 σ^0 map, acquired when the snowpack surface was likely dry as determined from air temperature data (see Fig. 11a & b). (Note also the location and outline of Mono Basin in Fig. 5.) Though these preliminary results are inconclusive, they are consistent with available literature indicating that there is a 3 – 5 dB drop in σ^0 from dry to wet snow.

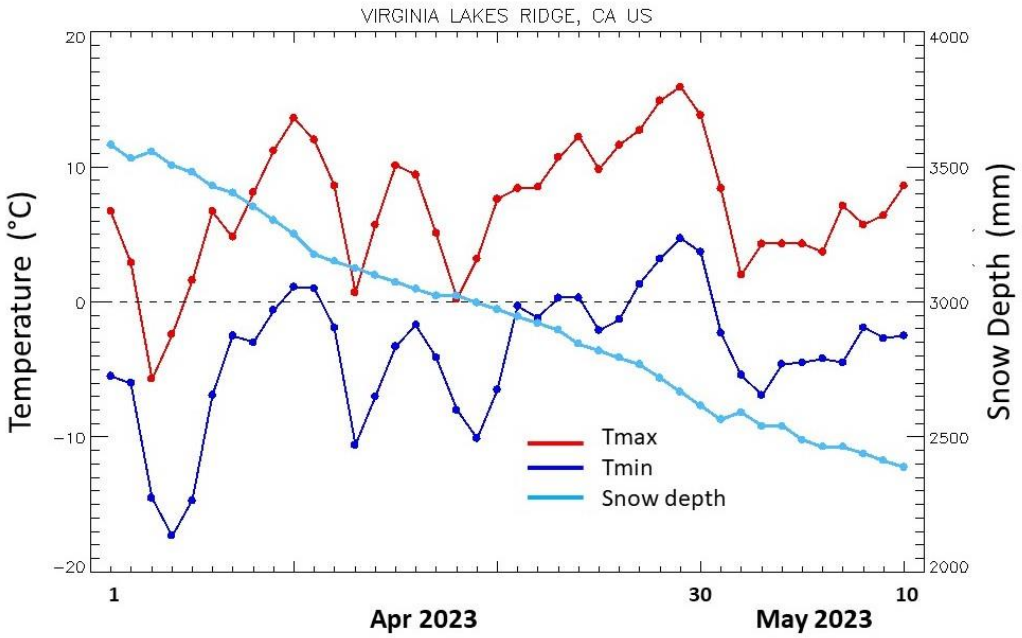

Figure 10. In the Sierra Nevada mts. study area (Fig. 3), Tmax at the Virginia Lakes Ridge station, northwest of Mono Lake, is consistently above 0°C from 5 April - 10 May 2023. Data acquired from SNOTEL (2022 - 2023).

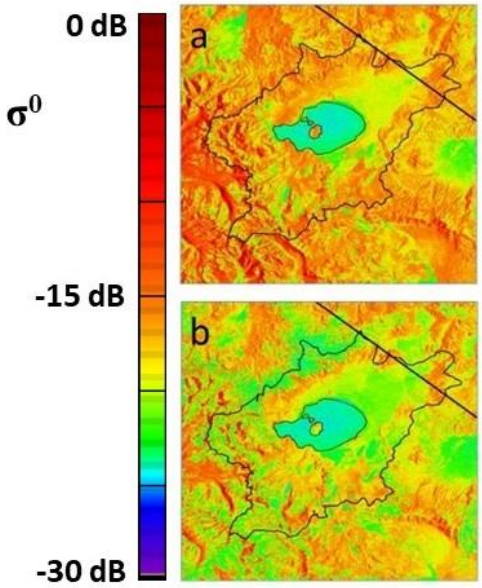

Figure 11. S-1a C-band SAR VH backscatter maps (ascending passes) focusing on Mono Basin. The thin black line delineates the basin. The thicker straight black line is the boundary line between California and Nevada. a) Acquired on 20 January 2023 when presumed dry snow covered the entire area; b) Acquired on 8 May 2023 during active snowmelt (see Fig. 10). Note the lower overall backscatter in b) as compared to a), possibly due to active snowmelt on 8 May.

DISCUSSION AND CONCLUSION

The 1 December 2022 – 31 January 2023 time series of MODIS and VIIRS cloud-gap-filled snow maps did not adequately map snow over the persistently-cloudy study area in western New York

state because there were long stretches of time when the surface was not visible to optical sensors. The daily IMS snow maps are the most useful maps available for this study area during the fall and winter months due to the persistent clouds. In the SN study area over the 2022 – 2023 winter and spring, there were frequent views of the surface between storms and thus the MODIS and VIIRS cloud-gap-filled snow maps performed well for mapping snow there. In this paper, we show only results from IMS and VIIRS.

To map wet snow using C-band SAR data, a snow mask developed from optical data is needed (Nagler et al., 2008 and 2016; Solberg et al., 2016; Manickam & Barros, 2020). But even with an optically-derived snow mask, it may not be possible to map snow using C-band SAR data because of the similarity in backscatter, σ^0, between wet ground and wet snow. This is especially true when the snowpack is shallow and wet as was the case in western New York during our study period on the days for which S-1a C-band SAR data were available.

Specifically, we did not see a significant difference in σ^0 between snow-covered and non-snow-covered land areas in our study area in western New York from 1 December 2022 to 31 January 2023. Though we see a snowline on the 22 December scene on VIS/NIR imagery, the σ^0 does not change significantly above and below the snowline, even though many researchers have shown strong backscatter decreases (3 – 5 dB) between snow-free ground and wet snow in other study areas as discussed earlier. The reason that we are not seeing a σ^0 change is likely because the snow is wet and quite thin (mostly < 0.1 m) and the ground (mostly cropland) in the vicinity of the snow cover on 22 December 2022 is probably also wet based on reported Tmax temperatures. At C-band, backscatter from vegetation can significantly contribute to the total backscatter or even dominate the snow signature (Nghiem and Tsai, 2001).

To map both dry and wet snow using SAR data, higher microwave frequencies such as X/Ku-band have much more potential than C-band (e.g., Matzler, 1984). Backscatter from snow at Ku-band (~14 GHz) is 5.4 times stronger than at X-band (~9 GHz) and 40 times stronger compared to C-band (~5.3 GHz) (Nghiem and Tsai, 2001). Though there are many circumstances when the S-1a C-band SAR can map snow in conjunction with a VIS/NIR snow mask, it is not universally possible according to this preliminary work.

Acknowledgements. The authors thank HP Marshall/Boise State University, Thomas Nagler/Enveo IT GmbH, Austria, Ana Barros/University of Illinois and Surendar Manickam/Vellore Institute of Technology, India, for discussions about snow wetness and C-band SAR.

REFERENCES

Baghdadi N, Gauthier Y, Bernier M., Fortin JP. 2000. Potential and limitations of RADARSAT SAR data for wet snow monitoring. *IEEE Transactions on Geoscience and Remote Sensing,* **38**: 316-320.

Bernier M, Fortin JP. 1998. The Potential of Times Series of C-Band SAR Data to Monitor Dry and Shallow Snow Cover. *IEEE Transactions on Geoscience and Remote Sensing,* **36**: 226-243.

Bernier M, Fortin JP, Gauthier Y, Gauthier R, Roy R, Vincent P. 1999. Determination of snow water equivalent using RADARSAT SAR data in eastern Canada. *Hydrological Processes,* **13**: 3041-3051.

ESA. 2023. Sentinel-1 C-band Synthetic Aperture Radar (SAR), *https://www.earthdata.nasa.gov/sensors/sentinel-1-c-band-sar*

Friedl M, Sulla-Menashe D. 2019. MCD12Q1 MODIS/Terra+Aqua Land Cover Type Yearly L3 Global 500m SIN Grid V006 [Data set]. NASA EOSDIS Land Processes DAAC. Accessed 2023-03-16 from *https://doi.org/10.5067/MODIS/MCD12Q1.006*

GIBS (Global Imagery Browse Services) NASA Worldview. 2004. *https://worldview.earthdata.nasa.gov/*

Hall DK, Riggs GA. 2020. MODIS/Terra CGF Snow Cover Daily L3 Global 500m SIN Grid, Version 61 [dataset]. Boulder, Colorado USA. NASA National Snow and Ice Data Center Distributed Active Archive Center. *https://doi.org/10.5067/MODIS/MOD10A1F.061*

Helfrich S, Li M, Kongoli C, Nagdimunov L, Rodriguez E. 2018. IMS Algorithm 991 Theoretical Basis Document Version 2.4. 74.

Lievens H, Brangers I, Marshall H-P, Jonas T, Olefs M, De Lannoy G. 2022. Sentinel-1 snow depth retrieval at sub-kilometer resolution over the European Alps. *The Cryosphere*, **16:** 159–177.

Lund J, Forster RR, Deeb EJ, Liston GE, Skiles SM, Marshall H-P. 2022. Interpreting

Sentinel-1 SAR backscatter signals of snowpack surface melt/freeze, warming, and ripening through field measurements and physically-based SnowModel. *Remote Sensing*, **14**: 4002. *https://doi.org/10.3390/rs14164002*

Manickam S, Barros A. 2020. Parsing synthetic aperture radar measurements of snow in complex terrain: Scaling behaviour and sensitivity to snow wetness and landcover. *Remote Sensing*, **12:** 483. *https://doi:10.3390/rs12030483*.

Marin C, Bertoldi G, Premier V, Callegari M, Brida C, Hürkamp K, Tschiersch J, Zebisch M, Notarnicola C. 2020. Use of Sentinel-1 radar observations to evaluate snowmelt dynamics in alpine regions. *The Cryosphere*, **14**: 935–956.

Mätzler C, Schanda E. 1984. Snow mapping with active microwave sensors. *International Journal of Remote Sensing*, **5**: 409-422.

Mätzler C. 1987. Applications of the interaction of microwaves with the natural snow cover. *Remote Sensing Reviews*, **2**: 259-387.

NASA Worldview. (2022 - 2023). *https://worldview.earthdata.nasa.gov/*

NCEI. 2023. NOAA National Centers for Environmental Information, Daily Summaries Version 3.1.0, Global Historical Climate Network includes daily land surface observations from around the world [Dataset]. *https://www.ncei.noaa.gov/maps/daily-summaries/*

Nagler T, Rott H. 2000. Retrieval of wet snow by means of multitemporal SAR data. *IEEE Transactions on Geoscience and Remote Sensing*, **38**: 754-765.

Nagler T, Rott H, Malcher P, Muller F. 2007. Assimilation of meteorological and remote sensing data for snowmelt runoff forecasting. *Remote Sensing of Environment*, **112**: 1408-1420. *https://doi:10.1016/j.rse.2007.07.006*

Nagler T, Rott H, Ripper E, Bippus G, Hetzenecker M. 2016. Advancements for snowmelt monitoring by means of Sentinel-1 SAR. *Remote Sensing*, **8**: 348.

Nghiem SV, Tsai WY. 2001. Global snow cover monitoring with spaceborne Ku-band scatterometer. *IEEE Transactions on Geoscience and Remote Sensing*, **39**: 2118-2134.

NSIDC. 2023. *https://nsidc.org/data/viirs/data#top*

Riggs GA, Hall DK, Román MO. 2019. MODIS Snow Products Collection 6.1 User Guide Version 1. *http://modis-snow-ice.gsfc.nasa.gov/?c=userguides*

Riggs GA, Hall DK. 2021. NASA S-NPP VIIRS Snow Cover Products Collection 2 User Guide. *http://modis-snow-ice.gsfc.nasa.gov/?c=userguides*

Riggs GA, Hall DK, Román MO. 2019. VIIRS/NPP Snow Cover Daily L3 Global 375m SIN Grid, Version 1 [dataset]. Boulder, Colorado USA. NASA National Snow and Ice Data Center Distributed Active Archive Center. *https://doi.org/10.5067/VIIRS/VNP10A1.001*

Riggs GA, Hall DK. 2020. Continuity of MODIS and VIIRS snow cover extent data products for development of an Earth Science Data Record. *Remote Sensing*, **12**: 3781. *https://nsidc.org/sites/nsidc.org/files/technical-references/Riggs&Hall.2020.pdf*

Rott H, Davis RE, Dozier J. 1992. Polarimetric and multifrequency SAR signatures of wet snow. *Proceedings of the Internationl Geoscience and Remote Sensing Symposium* (26-29 May, 1992, Houston, Texas, USA): 1658-1660.

Sentinel-1 SAR. 2018. IEEE International Geoscience and Remote Sensing Symposium, Publisher: IEEE, 2018:8727-8730, *https://doi.10.1109/IGARSS.2018.8518203*, ISBN: 978-1-5386-7150-4.

SNOTEL. 2022 – 2023. USDA SNOTEL data for Virginia Lakes Ridge, California *https://wcc.sc.egov.usda.gov/nwcc/site?sitenum=846*

Solberg R, Rudjord Ø, Salberg AB, Due Ø, Trier GS, Diamandi A, Irimescu A. 2016. Single-and multi-sensor snow wetness mapping by Sentinel-1 and MODIS data. *73rd Eastern Snow Conference*, Columbus, OH.